

## Spontaneous Reduction of Metal Ions Initiated by Ethylenediamine-Capped CdS Nanowires: A Sensing Mechanism Revealed

Yung-Jung Hsu,<sup>\*,†</sup> Shih-Yuan Lu,<sup>\*,‡</sup> and Yi-Feng Lin<sup>‡</sup>

Department of Materials Science and Engineering, National Chiao Tung University, Hsinchu, Taiwan 30010, Republic of China, and Department of Chemical Engineering, National Tsing Hua University, Hsinchu, Taiwan 30013, Republic of China

Received October 26, 2007

Revised Manuscript Received January 23, 2008

Nanostructured semiconductors have drawn much research attention in the recent two decades due to their unique application edges in optoelectronics. In particular, they are very attractive fluorescent probe materials for chemical species and possess the advantages of narrow spectral bandwidth, tunable emission wavelength, and photochemical stability as compared to conventional dyes.<sup>1</sup> A wide range of semiconductor-based fluorescence sensors have thus been developed to detect specific chemical species. Among them, the detection of silver and copper ions is particularly relevant to the development of biology and immunology and has drawn much research attention in recent years.<sup>2</sup> The detection of a specific ion relies on the quenching or enhancing effect of the ion on the fluorescence intensity of the host semiconductor. Such quenching or enhancing effect was often loosely attributed to the electron transfer or surface passivation process, respectively.<sup>2,3</sup> To further the development on semiconductor-based chemical sensors, a more rigorous understanding on the sensing mechanism is needed. In this work, the sensing mechanism of ethylenediamine (EN)-capped CdS nanowires (NWs) toward Ag<sup>+</sup> and Cu<sup>2+</sup> ions was revealed with a direct observation of the side product of the sensing event. For Ag<sup>+</sup> or Cu<sup>2+</sup> ions, the binding of the ions to and subsequent redox at the surfaces of the CdS NWs trigger an in situ growth of the corresponding metal nanoparticles on the NW surfaces and affect the transduction of the binding event into an optical signal that can be readily observed and quantified. The success of the present work

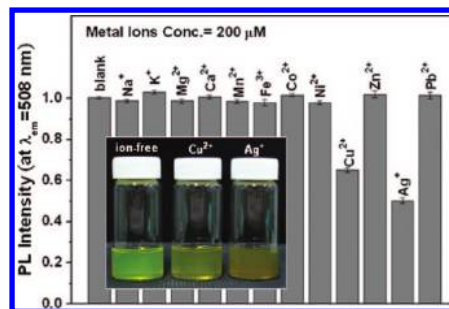


**Figure 1.** Effect of exposure to 12 metal ions on PL of EN-capped CdS NWs. The concentrations of metal ions and NWs were 200 μM and 5.8 × 10<sup>-4</sup> M, respectively. The inset shows the color difference among the ion-free and Cu<sup>2+</sup>- and Ag<sup>+</sup>-containing NW samples.

was made possible by using NWs as the sensing host, instead of nanoparticles commonly used in literature, through which the side products of the sensing event can be clearly observed and characterized on this one-dimensional platform.

The photoluminescence (PL) responses of the EN-capped CdS NWs as exposed to 12 commonly encountered, physiologically relevant metal ions were first compared to identify the sensible species. The PL of the ion-free NW sample was taken as the control. As shown in Figure 1, the PL interferences resulting from the presence of all but silver and copper ions, at a rather high concentration of 200 μM, were negligibly small. The PL intensity of the CdS NWs was however quenched by 59% and 35% in the solutions containing Ag<sup>+</sup> and Cu<sup>2+</sup>, respectively. In addition to the PL quenching, the color of the samples, upon addition of Ag<sup>+</sup> or Cu<sup>2+</sup>, changed rapidly in an extent that even the naked eye can recognize, from shiny yellow for ion-free to brown for Ag<sup>+</sup> and to brownish yellow for Cu<sup>2+</sup> samples, as shown in the inset of Figure 1. The apparent color change was due to the presence of Ag or Cu nanocrystals on the NW surfaces, resulting from a spontaneous reduction of the relevant ions.

Figure 2a,b shows the scanning electron microscope (SEM) images of the Ag<sup>+</sup>- and Cu<sup>2+</sup>-treated CdS NWs, respectively. A large quantity of nanoparticles, with a size of 10–15 nm as evident from Figure 2c,e, were present on the NW surfaces. The transmission electron microscope–energy dispersive spectrometry (TEM-EDS) line scans, shown in the insets of Figure 2c,e, reveal that these nanoparticles were Ag and Cu for the Ag<sup>+</sup>- and Cu<sup>2+</sup>-treated CdS NWs, respectively. Furthermore, the amount of sulfur detected in the domain of the surface-attached particle was negligible, giving solid proof that the grown particle was pure metal instead of sulfide. Figure 2d,f further shows the detailed crystallographic structures of the nanoparticles and NWs at the interface area with high-resolution TEM (HRTEM) images. In Figure 2d, an HRTEM image taken on the interface of the CdS NW and nanoparticle clearly reveals two distinct sets of lattice fringes. An interlayer spacing of 0.67 nm was observed in the NW region, in good agreement with the *d* spacing of the (0001) lattice planes of the hex-

\* Corresponding author. E-mail: yhsu@cc.nctu.edu.tw (Y.-J.H.); sylu@mx.nthu.edu.tw (S.-Y.L.).

<sup>†</sup> National Chiao Tung University.

<sup>‡</sup> National Tsing Hua University.

- (1) (a) Bruchez, M. J.; Moronne, M.; Gin, P.; Weiss, S.; Alivisatos, A. P. *Science* **1998**, *281*, 2013. (b) Chan, W. C. W.; Nie, S. M. *Science* **1998**, *281*, 2016. (c) Han, M. Y.; Gao, X. H.; Su, J. Z.; Nie, S. M. *Nat. Biotechnol.* **2001**, *19*, 631. (d) Mattoussi, H.; Manro, J. M.; Goldman, E. R.; Anderson, G. P.; Sundar, V. C.; Mikula, F. V.; Bawendi, M. G. *J. Am. Chem. Soc.* **2000**, *122*, 12142.
- (2) (a) Chen, Y.; Rosenzweig, Z. *Anal. Chem.* **2002**, *74*, 5132. (b) Gattas-Asfura, K. M.; Leblanc, R. M. *Chem. Commun.* **2003**, 2684. (c) Liang, J.-G.; Ai, X.-P.; He, Z.-K.; Pang, D.-W. *Analyst* **2004**, *129*, 619. (d) Tang, B.; Niu, J.; Yu, C.; Zhuo, L.; Ge, J. *Chem. Commun.* **2005**, 4184. (e) Konishi, K.; Hiratani, T. *Angew. Chem., Int. Ed.* **2006**, *45*, 5191.
- (3) (a) Spanhel, L.; Haase, M.; Weller, H.; Henglein, A. *J. Am. Chem. Soc.* **1987**, *109*, 5649. (b) Moore, D. E.; Patel, K. *Langmuir* **2001**, *17*, 2541.

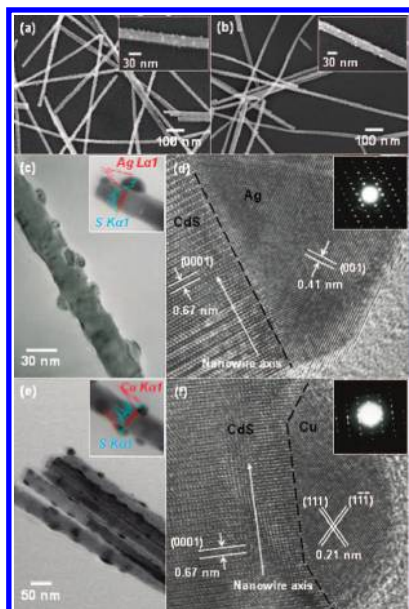


**Figure 2.** (a, b) SEM images of  $\text{Ag}^+$ - and  $\text{Cu}^{2+}$ -treated CdS NWs, respectively. (c) TEM and (d) HRTEM images taken on  $\text{Ag}^+$ -treated CdS NW. (e) TEM and (f) HRTEM images taken on  $\text{Cu}^{2+}$ -treated CdS NWs. TEM-EDS line-scan results were inserted in (c) and (d). Inserted in (d) and (f) were the corresponding SAED patterns. Metal ion concentration =  $200 \mu\text{M}$ .

agonal CdS crystal,<sup>4</sup> while in the particle region an interlayer spacing of  $0.41 \text{ nm}$  was obtained, complying with the lattice spacing of the (001) planes of the fcc Ag.<sup>5</sup> Similarly, for the  $\text{Cu}^{2+}$ -treated NW sample, the two lattice fringes observed in the regions of NW and nanoparticle correspond well to the (0001) and (111) lattice planes of the hexagonal CdS and fcc Cu,<sup>6</sup> respectively. Note that no oxide layer can be observed on the surfaces of the Ag and Cu nanoparticles, indicating that the products did not suffer from oxidation. The corresponding electron diffraction (ED) patterns, shown in the insets of Figure 2d,f, further verify the presence of Ag and Cu nanocrystals, with the dot patterns contributed by the single crystalline CdS NWs and ring patterns by the Ag and Cu nanocrystals. This result, together with those of the HRTEM, TEM-EDS, and X-ray photoelectron spectroscopy (XPS, Figure S1 and Figure S2, Supporting Information) analyses, confirms the formation of Ag and Cu nanocrystals on the NW surfaces upon addition of  $\text{Ag}^+$  and  $\text{Cu}^{2+}$ , respectively.

We attribute the formation of the Ag and Cu nanocrystals to the reduction of the added  $\text{Ag}^+$  and  $\text{Cu}^{2+}$ , occurring at the surfaces of the CdS NWs. The as-prepared CdS NWs were coated with a thin layer of EN which served as the capping reagent during the NW synthesis. EN however has also been shown to have strong coordination with metal ions and can work as a weak reducing reagent.<sup>7</sup> Upon addition of the tested metal ions, the CdS NWs may coordinate with the metal ions through the chelating characteristics of EN, as illustrated in Figure S3, Supporting Information. Among the 12 metal ions tested in this work, only  $\text{Ag}^+$  and  $\text{Cu}^{2+}$

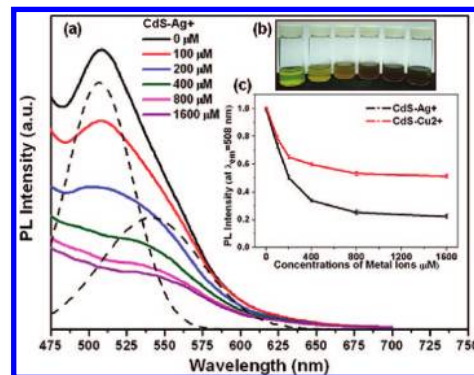


**Figure 3.** (a) PL and (b) color change of CdS NWs samples upon addition of  $\text{Ag}^+$  at five increasing concentrations. In (b), the concentrations of  $\text{Ag}^+$  from left to right were 0 to  $1600 \mu\text{M}$ . (c) Quenching of excitonic emission with increasing metal ion concentration.

possess positive standard reduction potentials ( $E^\circ(\text{Ag}^+ - \text{Ag}) = 0.80 \text{ V}$ ,  $E^\circ(\text{Cu}^{2+} - \text{Cu}) = 0.34 \text{ V}$ ), signifying that  $\text{Ag}^+$  and  $\text{Cu}^{2+}$  have a higher tendency to be reduced, as compared to the other tested ions, because of their stronger electron affinity. As a result, EN reduced the chelated  $\text{Ag}^+$  and  $\text{Cu}^{2+}$  to form Ag and Cu nanoparticles on the NW surfaces. It is important to note that the reduction did not proceed without the presence of the CdS NWs, implying that the CdS NWs are an indispensable initiator for the reduction of  $\text{Ag}^+$  and  $\text{Cu}^{2+}$  with EN.

Figure 3 shows the PL responses of the CdS NW solutions toward the addition of  $\text{Ag}^+$  at five increasing concentrations. The PL spectra exhibit a major emission band at  $508 \text{ nm}$ , a typical excitonic band-to-band radiative emission of CdS,<sup>8</sup> and a minor shoulder at  $550 \text{ nm}$ , a shallow defect level emission,<sup>9</sup> as can be more clearly seen with the PL peak deconvolution. At the  $\text{Ag}^+$  concentration of  $400 \mu\text{M}$ , the excitonic emission of the NWs was quenched to an extent that the shallow defect level emission became dominant.

Figure 3c depicts the concentration dependence of the luminescence intensity of the CdS NWs. The intensity of the excitonic emission decreases sharply with increasing ion concentration and then levels off when the ion concentration reaches  $800 \mu\text{M}$ , exhibiting the typical Stern–Volmer quenching behavior.<sup>10</sup> In addition to the PL quenching, the color change of the NW solutions was also evident, turning darker brown with increasing  $\text{Ag}^+$  concentration as illustrated in Figure 3b. Note that the color of the NW solutions turns brown because of the strong surface plasma resonance of Ag nanocrystals present on the NW surfaces,<sup>11</sup> by which the solution became darker brown with increasing addition of  $\text{Ag}^+$ . The UV–visible absorption behavior of the CdS NWs in the presence of metal ions other than  $\text{Ag}^+$  and  $\text{Cu}^{2+}$  did not show any significant variation from the ion-free

(4) For bulk hexagonal CdS,  $d(0001) = 0.6713 \text{ nm}$  from JCPDS No. 06-0314.

(5) For bulk fcc Ag,  $d(100) = 0.4086 \text{ nm}$  from JCPDS No. 04-0783.

(6) For bulk fcc Cu,  $d(111) = 0.2087 \text{ nm}$  from JCPDS No. 04-0836.

(7) Lu, Q.; Gao, F.; Komarneni, S. *J. Mater. Res.* **2004**, *19*, 1649.

(8) (a) Hsu, Y.-J.; Lu, S.-Y. *Langmuir* **2004**, *20*, 23. (b) Hsu, Y.-J.; Lu, S.-Y.; Lin, Y.-F. *Adv. Funct. Mater.* **2005**, *15*, 1350.

(9) (a) Li, X.; Coffey, J. L. *Chem. Mater.* **1999**, *11*, 2326. (b) Liu, S.-M.; Liu, F.-Q.; Guo, H.-Q.; Zhang, Z.-H.; Wang, Z.-G. *Solid State Commun.* **2000**, *115*, 615.

(10) Lakowicz, J. R. *Principles of Fluorescence Spectroscopy*; Plenum Press: New York, 1983; Chapter 9, p 257.

(11) (a) Zhang, Q. F.; Liu, W. M.; Xue, Z. Q.; Wu, J. L.; Wang, S. F.; Wang, D. L.; Gong, Q. H. *Appl. Phys. Lett.* **2003**, *82*, 958. (b) Maddanimath, T.; Kumar, A.; D'Arcy-Gall, J.; Ganesan, P. G.; Vijayamohan, K.; Ramanath, G. *Chem. Commun.* **2005**, 1435.

samples. For  $\text{Ag}^+$  and  $\text{Cu}^{2+}$ -treated samples, the surface plasma resonance absorption of the corresponding metal nanocrystals was revealed and interfered with the excitonic absorption of the NWs, resulting in changes in the apparent colors of the solutions (as shown in Figure 1). Figure S4, Supporting Information, shows the absorption characteristics of the CdS NWs upon addition of  $\text{Ag}^+$  at five increasing concentrations. The absorption shoulder located at around 370 nm, attributable to the surface plasma resonance of the Ag nanocrystals,<sup>12</sup> became pronounced and interfered with the excitonic absorption of the NWs at  $\text{Ag}^+$  concentrations larger than 200  $\mu\text{M}$ . At a  $\text{Ag}^+$  concentration of 400  $\mu\text{M}$ , the absorption interference between the Ag nanocrystals and the NWs became so acute that the excitonic absorption of the NWs leveled off at the wavelength range of 300 to 450 nm. These phenomena, observed also for the  $\text{Cu}^{2+}$ -treated CdS NW solutions, can be explained with the in situ formation of Ag (or Cu) nanocrystals from the spontaneous reduction of  $\text{Ag}^+$  (or  $\text{Cu}^{2+}$ ) initiated by the EN-capped CdS NWs. It should be noted that the absorption characteristics of the CdS NWs were not affected when exposed to the other tested ions, since no corresponding metal nanocrystals were formed on the NW surfaces. As the concentration of these metal ions was further increased, the NWs suffered significant aggregation because of the strong metal-ion-EN complexing as discussed and demonstrated in Figure S3, Supporting Information. With increasing  $\text{Ag}^+$  concentration, there is an increasing amount of Ag formed on the surfaces of the CdS NWs. As shown in Figure S5, Supporting Information, the reduction-derived metal nanocrystals grew larger with increasing metal ion concentration. The larger size of the metal nanocrystals is responsible for the further suppression in PL intensity. We depicted the correlation of  $\text{Ag}^+$  concentrations with the extent of PL depression and the size of the resulting Ag nanocrystals in Figure S5g, Supporting Information. Such a phenomenon has been reported in a Au-CdSe system, in which Au nanoparticles selectively grew on tips of CdSe nanorods because of the preferred reaction occurring at the exposed nanorod tips.<sup>13</sup> The Au nanoparticles were found to grow larger in size with increasing Au precursors, which in turn promoted the coupling effect between Au and CdSe and resulted in more pronounced influence on the corresponding optical characteristics.

The in situ formed Ag nanocrystals can serve as an effective electron scavenger for the CdS NWs. The Fermi levels of both Ag and Cu are located at around +0.15 V versus NHE, lower in the energetic state than the conduction band of CdS (-1.0 V vs NHE).<sup>14</sup> Consequently, the photon-excited free electrons of CdS NWs would transfer to the metal domain in contact with the NWs, leading to depletion

of free electrons in the NW domain and subsequent suppression of the excitonic emission. It should be stressed that no interference in ion reduction was observed at cofeeding of  $\text{Ag}^+$  and  $\text{Cu}^{2+}$ . From the TEM-EDS analyses of Figure S6, Supporting Information, distinguishable nanoparticles of Ag and Cu were randomly attached on the NW host. This phenomenon further demonstrates the feasibility of using such EN-capped CdS NWs as nanoprobe for metal ions. In addition, standard deviations of the PL intensities obtained from five repeated measurements of a NW solution containing 100  $\mu\text{M}$  of  $\text{Ag}^+$  and  $\text{Cu}^{2+}$  are 1.7% and 1.6%, respectively, showing high reproducibility and applicability of the current system. As a final note, although the study was conducted at relatively high metal ion concentrations, the detection limits of the present NW system toward  $\text{Ag}^+$  and  $\text{Cu}^{2+}$  can be as low as  $4.9 \times 10^{-6}$  M and  $6.0 \times 10^{-6}$  M, respectively, as estimated from the corresponding blank tests and data presented in Figure 3c.<sup>15</sup> It might be argued that the spontaneous reduction of  $\text{Ag}^+$  and  $\text{Cu}^{2+}$  may be invoked by photogenerated free electrons from the CdS NWs instead of by EN molecules. To clarify this issue, a trivial experiment was conducted by incubating EN-capped CdS NWs in cysteine (Cys) solution to prepare Cys-capped CdS NWs. Note that cysteine is a nonreducing capping reagent.<sup>2a</sup> The corresponding PL response toward the addition  $\text{Ag}^+$  and  $\text{Cu}^{2+}$  ions was depicted in Figure S7, Supporting Information. It can be clearly seen that no significant PL depression occurred for the Cys-capped CdS NWs upon addition of  $\text{Ag}^+$  and  $\text{Cu}^{2+}$ . This demonstration supports our argument that EN molecules act as the reducing agent in our system to invoke the reduction of  $\text{Ag}^+$  and  $\text{Cu}^{2+}$ . This result also rules out the possibility that photogenerated free electrons from CdS NWs can work for the reduction of  $\text{Ag}^+$  and  $\text{Cu}^{2+}$  in this work.

In summary, the sensing mechanism of EN-capped CdS NWs toward  $\text{Ag}^+$  ( $\text{Cu}^{2+}$ ) was revealed with a direct observation of the side product of the sensing event, Ag (Cu) nanocrystals from the spontaneous reduction of  $\text{Ag}^+$  ( $\text{Cu}^{2+}$ ) by EN-capped CdS NWs. The CdS NWs not only provided an easily detectable platform for the direct observation of the sensing event product but also played an important initiating role in the reduction of  $\text{Ag}^+$  ( $\text{Cu}^{2+}$ ) ions. The associated rapid color change and moderately low detection limits make EN-capped CdS NWs an effective sensing host for metal ions in biological media.

**Acknowledgment.** This work was financially supported by the National Science Council of the Republic of China (Taiwan) under Grants NSC-96-2218-E-009-007 (Y.-J.H.) and NSC-95-2221-E-007-194 (S.-Y.L.).

**Supporting Information Available:** Experimental details, XPS spectra, TEM images, UV-visible spectra, photoluminescence spectra, and TEM-EDS analyses (PDF). This material is available free of charge via the Internet at <http://pubs.acs.org>.

CM7030703

- (12) Noguez, C. *J. Phys. Chem. C* **2007**, *111*, 3806.  
(13) (a) Mokari, T.; Rothenberg, E.; Popov, I.; Costi, R.; Banin, U. *Science* **2004**, *304*, 1787. (b) Mokari, T.; Szturum, C. G.; Salant, A.; Rabani, E.; Banin, U. *Nat. Mater.* **2005**, *4*, 855.  
(14) (a) Kamat, P. V.; Shanghavi, B. *J. Phys. Chem. B* **1997**, *101*, 7675. (b) Wood, A.; Giersig, M.; Mulvaney, P. *J. Phys. Chem. B* **2001**, *105*, 8810.

- (15) Gabriels, R. *Anal. Chem.* **1970**, *42*, 1439.